Solvent-Induced Frequency Shifts as a Probe for Studying Very Weak Molecular Complexes: Evidence for van der Waals Complex Formation between COF_2 and N_2 in Cryogenic Solutions

A. A. Stolov,† W. A. Herrebout, and B. J. Van der Veken*

Department of Chemistry, Universitair Centrum Antwerpen, Groenenborgerlaan 171, B2020 Antwerp, Belgium

Received: April 21, 1999

FTIR (4000−400 cm^{-1}) spectra of COF_2 dissolved in liquefied argon (LAr), krypton (LKr), xenon (LXe), nitrogen (LN_2), and in LAr/LN_2 mixtures have been investigated. In addition, spectra of COF_2 and COF_2/N_2 mixtures isolated in solid argon matrices have been studied. Vibrational frequencies of COF_2 dissolved in LN_2 exhibit unusual temperature behavior as compared to the solutions in the other solvents. This, and the effects on the vibrational frequencies and IR band shapes of COF_2 in mixed nitrogen/argon solvents, is attributed to the formation of a complex $COF_2 \cdot N_2$ in the solutions. A phenomenological model is proposed for the calculation of the temperature and concentration effects on the vibrational frequencies. By fitting the experimental data, the complexation enthalpy, $\Delta H° = -1.4(3)$ kJ mol^{-1}, was determined from this model. The existence of a $COF_2 \cdot N_2$ complex was confirmed by the matrix isolation spectra. Geometry, energy, and vibrational spectrum of $COF_2 \cdot N_2$ have been calculated by ab initio at the MP2/6-311++G(2d,2p) level. The ab initio predictions for $\Delta H°$ and for the complexation shifts of the vibrational bands agree well with the values determined from the phenomenological model.

Introduction

Intermolecular attractions are the driving force for the formation of molecular complexes. When the interactions are very weak, the complexes belong to the realm of the van der Waals adducts. In recent years the formation of such adducts between weak Lewis acids and bases has been intensely studied in cryosolutions, using liquid argon (LAr) and liquid nitrogen (LN_2) as solvents.[1−6] The solutions were investigated using infrared spectroscopy, and the formation of complexes invariably was deduced from the occurrence of new vibrational bands in the spectra that could not be attributed to the monomers. The complexation enthalpies found for these complexes typically were in excess of 4 kJ mol^{-1}. During these studies it was observed that in LN_2 some monomers such as HCl[7] and BF_3[8] are engaged in complexes with the solvent molecules. Especially for the latter, the interaction with the solvent significantly influences its behavior.[8] Hence, the study of these complexes is of some importance. The detection of a complex is straightforward when separate monomer and complex bands are observed. A condition for this is that the average lifetime of the complex is long compared with the period of the vibrations studied. For very weak complexes, however, this can become a problem, as can be seen as follows.

The lifetime of a complex, τ, can be estimated using the Arrhenius equation:

$$\tau^{-1} = A \exp(-\Delta E^*/RT) \qquad (1)$$

where the preexponential A falls in the range of $10^{13}-10^{14}$ s^{-1}, and ΔE is the activation energy, which for the complexation reaction is of the order of $\Delta H°$, the complexation enthalpy. If at the conditions of experiment the latter is about 1.5 kJ mol^{-1}, then, taking $T \approx 100$ K as in the cryosolutions, the magnitude of τ falls between 6×10^{-14} and 6×10^{-13} s, that is, τ is of the order of 10^0-10^1 periods of intra- or intermolecular vibrations. It is obvious that at such low lifetimes the complex species will not be able to produce a vibrational spectrum separated from that of the monomers. The presence in the cryosolutions of such weak complexes can, therefore, only be inferred from indirect evidence. This evidence, by necessity, can only be drawn from the observed band frequencies and band shapes.

Solvent-induced frequency shifts have been the object of study for many years, and different theoretical approaches have been developed for predicting their magnitudes.[9−19] It is generally acknowledged that intramolecular frequency shifts are determined by the normal coordinate-dependent parts of the attractive and repulsive interactions between the solute and the solvent.[9−14] The attractive interactions may contain contributions from electrostatic, dispersive, and specific forces.[14,21] Theoretical descriptions of frequency shifts, in the absence of complexation, are based on different simplifications. An extensively developed approach is based on the hard-sphere fluid model.[10−14] In this, the contribution of repulsive interactions is calculated from the solvation mean force exerted along the bond axis of the hard-sphere diatomic solute. The contribution of attractive interactions is usually obtained by fitting the experimental shifts at ambient conditions, and assuming that this contribution is linearly related to the density of the fluid. Several approaches are based on applying Onsager-type continuum models,[15−21] in which the relative permittivity of the solvent, κ, plays a central role. In this field, the Kirkwood−Bauer−Magat (KBM) formula[15] gives a useful correlation[20] between observed vibrational frequencies and the Kirkwood function, $\chi = (\kappa - 1)/(2\kappa + 1)$. Complexation of the solute with the solvent is known[22] to cause deviations from continuum-theory predictions. Previous studies on these

* Corresponding author. E-mail: bvdveken@ruca.ua.ac.be.
† Permanent address: Polymer Science and Engineering Department, Conte Building, University of Massachusetts, Amherst, MA 01003.

10.1021/jp991308j CCC: $18.00
Published on Web 06/19/1999

TABLE 1: Frequencies and Frequency Shifts (cm^{-1}) for Some Modes of COF_2 in Different Media

		solution−vapor frequency shift							
Mode[a]	ν_{vap}	LAr/110 K	LKr/160 K	LXe/220 K	LN_2/90 K	$\nu_{matrix(mon)}$	$\nu_{matrix(comp)}$	$\nu_{calc(mon)}$	$\nu_{calc(comp)}$
ν_1	1944.10	−7.69	−9.22	−9.99	−5.66	1941.2	1942.4	1945.3	1946.8
ν_2	962.69	−1.98	−2.40	−2.98	−0.18	965.3	966.8	957.1	958.1
ν_3	581.52	−1.04	−1.26	−1.73	−0.35			585.1	586.5
ν_4	1242.88	−7.73	−8.84	−10.44	−3.35	1237.5	1238.7	1227.2	1229.5
ν_5	619.22	−0.77	−1.00	−1.66	+0.10			621.9	622.0
ν_6	774.05	−3.69	−4.45	−5.92	−3.82	769.0	767.8	784.2	781.9
$2\nu_2$	1912.85	−5.02	−6.23	−7.85	−2.91	1913.2	1914.4		

[a] ν_1 is the C═O stretch, ν_2 is the CF_2 symmetric stretch, ν_3 is the COF_2 in-plane deformation, ν_4 is the CF_2 asymmetric stretch, ν_5 is the COF_2 in-plane asymmetric deformation, ν_6 is the COF_2 out-of-plane deformation.

deviations have concentrated on systems in which relatively strong complexes are formed. Then, either separate complex bands are observed, or the solute is virtually quantitatively complexed by the solvent, so that in the spectra only the complex bands are detected. Here, however, we are interested in a system from the other end of the scale, where a very weak complex is formed, and where, consequently, corresponding monomer and complex bands coalesce. This, as we try to prove in this study, occurs for solutions of carbonyl fluoride, COF_2, in LN_2 and in LAr/LN_2 mixtures. It is the aim of this paper to show that for these situations a phenomenological model can be set up, by which the observed frequencies can be described, and that allows that quantitative information on the complex is abstracted from the spectra.

Experimental Section

Carbonyl fluoride (CP grade) was obtained from Fluorochem Ltd (Old Glossop, Derbyshire, UK). The solvent gases Ar, Kr, Xe and N_2 were supplied by L'Air Liquide (Antwerpen, Belgium) and have a stated purity of 99.9999%, 99.998%, 99.995%, and 99.9999%, respectively. The carbonyl fluoride as obtained was found to contain $COCl_2$ (≈1%) and COClF (≈0.5%). Before use, the sample was purified on a low-pressure low-temperature fractionation column. The concentration of COF_2 in cryosolutions was approximately 1.4×10^{-4} M.

The infrared spectra were recorded on Bruker IFS 113v and Bruker IFS 66v interferometers, using a Globar source, a Ge/KBr beam splitter, and a broad band MCT detector. The interferograms were averaged over 200 scans, Blackman−Harris apodized, and Fourier transformed using a zero filling factor of 4, to yield spectra at a resolution of 0.5 cm^{-1}.

The cryosolution setup consists of a pressure manifold for filling and evacuating the cell and for monitoring the amount of solute gas used, and of the actual cell, machined from a massive brass block. The cell is equipped with wedged Si windows and has an optical path length of 40 mm. Details have been previously described.[1,23]

For the determination of peak positions, the IR band envelopes were fitted using Gauss−Lorentz sum functions, and in particular cases, using Voigt functions. All bands studied were found to be symmetric, and the center of the function was considered as the frequency of the band. The reproducibility of band centers, determined in this way, was not worse than ±0.02 cm^{-1}. This high reproducibility evidently is linked with the small bandwidths observed in cryosolutions, and with the inherent precision of Fourier transform spectrometers.

A Leybold Heraeus ROK 10−300 cryostat was used to obtain spectra of COF_2/N_2 mixtures isolated in argon matrices. The COF_2/Ar ratio was 1:900, whereas the N_2/Ar ratio was varied between 1:300 and 1:5. The sample was grown by vapor deposition on a CsI substrate cooled to 10 K. Deposition times were approximately 1 h.

Ab initio calculations were performed using *Gaussian94*.[24] For all calculations, electron correlation was accounted for by using Møller−Plesset perturbation theory including explicitly all electrons, whereas the Berny optimization[25] was used with the tight convergence criteria. A 6-311++G(2d,2p) basis set was used throughout as a compromise between accuracy and applicability to larger systems. The basis set superposition error (BSSE) was accounted for by the counterpoise method of Boys and Bernardi.[26] The vibrational frequencies and infrared intensities were calculated using harmonic force fields.

Results and Discussion

A. Spectra of Cryosolutions. The carbonyl fluoride molecule belongs to the point group C_{2v} and exhibits six normal vibrations, all of which are infrared active. The vapor phase frequencies obtained in this work are given in Table 1. They agree with those published by Mallinson et al.[27] The solvent-induced frequency shifts, defined as $\nu_{solution} - \nu_{gas}$, observed for solutions in LAr, liquid krypton (LKr), liquid xenon (LXe), and in LN_2, at the temperatures indicated, have been collected in Table 1. The data for the solutions in LAr agree with those of Shchepkin et al.[28]

The solvent-induced frequency shifts are the sum of attractive and repulsive contributions.[14] At high pressures ($P \sim 10^3-10^4$ bar) the repulsive term is larger than the attractive one,[11,12,14] but at the pressures used in this study, for all solvents used, the attractive contributions dominate. As a consequence, negative solvent frequency shifts must be expected. The results in Table 1 in general confirm this. The exception is ν_5 in LN_2, but this, as will be seen below, is attributed to the formation of a complex between the solute and nitrogen.

With increasing temperature, the density of cryosolvents decreases significantly.[29] Since the mean attractive force is proportional to the fluid density,[14] the absolute shifts become smaller when the temperature increases. In other words, positive slopes ($d\nu/dT$) have to be expected.

Figures 1−3 compare the influence of temperature on the band centers of some vibrations of COF_2 in LAr and LN_2. The slopes for ν_6 in LAr and LN_2 (Figure 1) and for ν_2 and ν_4 in LAr (Figures 2B and 3B) are positive, as expected. However, this is not the case for ν_2 and ν_4 in LN_2. It can be seen from Figure 2A that the frequency of ν_2 decreases with T, whereas for ν_4, the curve exhibits a minimum at approximately 98 K (Figure 3A).

The nonmonotonic temperature behavior of ν_4 proves that the observed solvent shift is the sum of two opposite contributions, whose relative importance is inversed in the temperature interval studied. The first contribution must be due to the decreasing density, and results in a red shift of the vibrational band. At the pressures used it is highly unlikely that the second contribution, the blue shift, is caused by changes in the repulsive

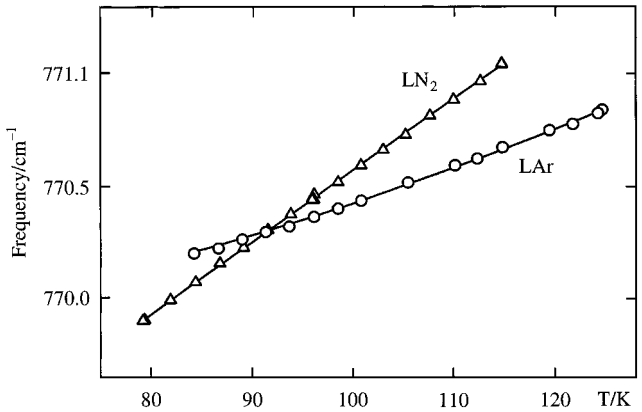

Figure 1. Frequency of ν_6 of COF_2 dissolved in LAr and LN_2, as a function of temperature.

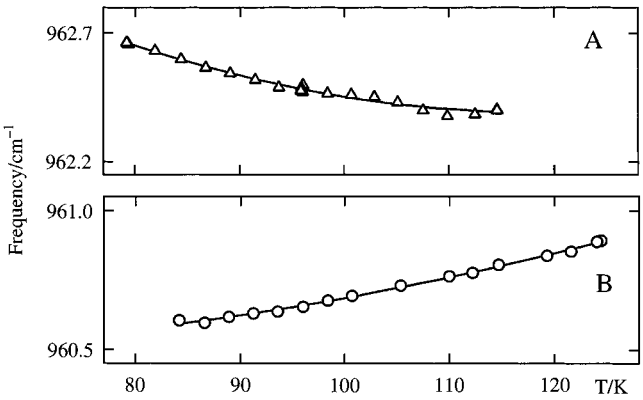

Figure 2. Frequency of ν_2 of COF_2 dissolved in (A) LN_2 and (B) LAr, as function of temperature.

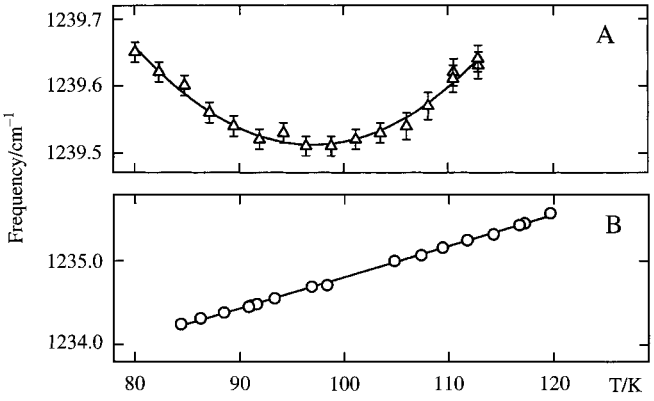

Figure 3. Frequency of ν_4 of COF_2 dissolved in (A) LN_2 and (B) LAr, as function of temperature.

contributions from the solvent molecules in the solvation shell. Therefore, we attribute the second contribution to the formation of a complex between COF_2 and N_2. This interpretation can only be correct if the frequency of ν_4 increases upon complexation, and if the observed band frequency is the average of the frequencies of ν_4 in monomer and complex. It will be seen below that the matrix isolation experiments and the ab initio calculations confirm the upward complexation shift for ν_4, whereas the model used to analyze the solvent frequency shifts, also described below, leads to a complexation enthalpy consistent with the coalescence of the monomer and complex bands. Within this interpretation, at lower temperatures the fraction of complexes increases, which eventually leads to the observed reversal in the temperature dependence.

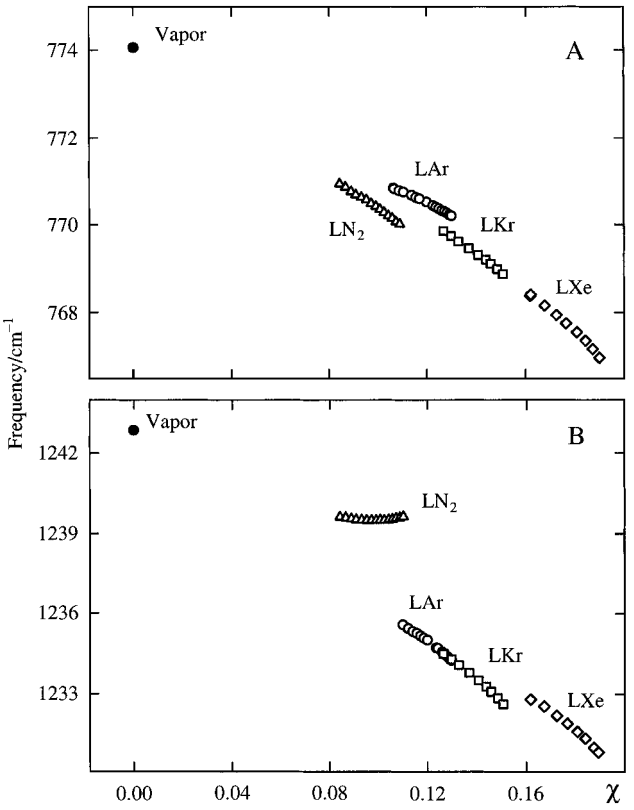

Figure 4. Correlation between the band frequency and the Kirkwood function of the solvent for (A) the ν_6 mode and (B) the ν_4 mode of COF_2.

The anomalous behavior of LN_2 as a solvent is further illustrated in Figures 4 and 5. In these, the band frequencies are plotted against the Kirkwood function of the solvents, $\chi = (\kappa - 1)/(2\kappa + 1)$, where κ is the relative permittivity of the medium. It is seen that for solutions in LAr, LKr, and LXe the relations $\nu = f(\chi)$ are close to linear, and their extrapolation to $\chi = 0$ neatly reproduces the vapor-phase frequencies. Such linear correlations, incorporating both the vapor- and condensed-phase data, are predicted by the KBM relation.[15,21] Although the data points in LAr, LKr, and LXe do not fall on a single straight line, the plots for these three solvents are close to each other.

The KBM plots for LN_2 solutions are nearly linear for ν_1, ν_6, and $2\nu_2$ of COF_2 (Figures 4A, 5A). In contrast, the plots for ν_2 and ν_4 are significantly nonlinear (Figures 4B, 5B). It should also be noted that the slopes of the LN_2 data for ν_2, ν_4, and $2\nu_2$ deviate significantly from those of the rare gas solutions data.

Deviations of experimental frequencies from the KBM relation are usually interpreted as a result of solute−solvent complex formation.[21,22] For the solutions in liquid nitrogen, this agrees with the hypothesis proposed above. At the same time it may be remarked that the linearity of the plots for the rare gases supports the proposition that no complexes are being formed between COF_2 and the rare gases.

The formation of a complex between COF_2 and N_2 can also be inferred from the study of COF_2 in mixed LAr/LN_2 solvents. The vibrational frequencies observed for ν_1, $2\nu_2$, ν_4, and ν_2, as function of temperature, in solvents in which the mole fraction of N_2 was 0.0, 0.096, 0.222, 0.416, 0.709, and 1.0, have been collected in Figure 6 (the continuous lines in the plots were obtained from calculations to be discussed below).

Using the data from Figure 6, the concentration dependence at constant temperature can be deduced. Some results for ν_4 and ν_6 are shown in Figure 7. The interaction of a solute

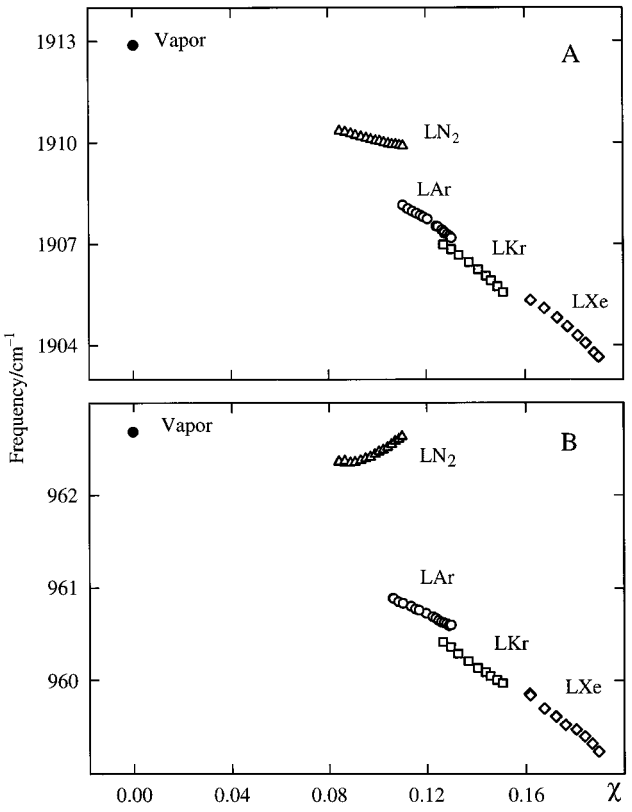

Figure 5. Correlation between the band frequency and the Kirkwood function of the solvent for (A) the $2\nu_2$ mode and (B) the ν_2 mode of COF_2.

molecule with its surrounding can be written[30] as a series in which the leading term contains the pairwise interactions, and subsequent terms contain three-body terms, four-body terms, etc. For the inert cryosolvent used in this study, this series converges rapidly, so that the first term dominates. In the pairwise approximation, in which only this first term is retained, the solvent shift of a solute vibration equals the sum of the shifts induced by each of the other molecules in the solution. Evidently, the dominant contributions will come from the molecules in the first solvation shell of the solute. Then, the total frequency shift must vary linearly with the mole fraction of nitrogen in the solute's solvation shell. If the Ar/N_2 ratio in the solvation shell equals the ratio in the bulk solvent, the plots in Figure 7 should be linear. However, the multiparticle interactions may upset this linearity. As nitrogen has a higher polarizability than argon, the multiparticle contributions will be more important for N_2 molecules of the solvation shell than for Ar atoms. As a consequence, deviations from linearity in Figure 7A due to multiparticle interactions should be more pronounced for high mole fractions of N_2 in the solvent. The figure, however, shows the opposite trend, that is, the strongest deviations occur for low mole fractions of N_2. Thus, the nonlinearity must be caused by a different phenomenon. There can be two reasons for this. First, preferential solvation with nitrogen can cause the mole fraction of nitrogen in the solvation shell to be higher than that in the bulk solvent, and, second, complexation will also upset the linearity. Some preferential solvation may take place, but Monte Carlo simulations for solutions of BF_3 in LAr/LN_2 mixtures have shown that the enrichment is relatively weak.[8] As BF_3 is rather similar to COF_2 (vide infra), it appears unlikely that the clear nonlinearities in Figure 7A are due to this. Simple manipulation of the equilibrium constant for a 1:1 complex $COF_2 \cdot N_2$ shows that the concentration of the complex increases more rapidly at low mole fractions of N_2 than at high values: this leads to a behavior as shown by the curves in Figure 7A. In view of these arguments, we prefer the interpretation that the nonlinearity in Figure 7A is the consequence of complexation.

Results similar to those of Figure 7A were also obtained for ν_1, ν_4, and $2\nu_2$. The behavior obtained for ν_6, shown in Figure 7B, however, is different: at lower temperatures the curves pass through a minimum, whereas at higher temperatures the frequency monotonically increases with the LN_2 concentration. The occurrence of a minimum, again, indicates that there are at least two mechanisms governing the band position, and, for the present case, at least one of the mechanisms must be temperature dependent. The behavior of the curves in Figure 7B can be explained by complex formation if the frequency of ν_6 decreases upon complexation. It will be seen below that this is confirmed by the matrix experiments and by the ab initio calculations.

A final indication for the complex formation was derived from a study of the band shape of ν_4. This band is well isolated from its neighbors, providing the opportunity for an accurate least-squares band fitting. The band profile of ν_4 was fitted in the region between 1275 and 1195 cm^{-1}, using a single Voigt function, that is, a convolution of a Lorentzian with a Gaussian function, for the present purpose defined as:

$$I(x) = \frac{1}{G}\left(\frac{\ln 2}{\pi}\right)^{1/2} \int_{-\infty}^{+\infty} \frac{\exp(-x_1^2)}{a^2 + (x - x_1)^2}\, dx_1$$

in which $a = (2 \ln 2)^{1/2}\, L/G$ and $x = (2 \ln 2)^{1/2}\, (\nu - \nu_o)/G$ with ν_o the band center, and G and L the half-width at half-maximum of the Gaussian and the Lorentzian contribution, respectively.

The analysis shows that the band is symmetric at all concentrations of LN_2 and at all temperatures but that the shape of the band varies with these parameters. According to the Kubo−Rothschild theory,[31] the Gaussian contribution to a band profile is mainly due to fluctuations in the environment of the molecules under study. The change of the Gaussian width δ_g with temperature and concentration depends on the average frequency fluctuation in the ensemble of molecules, and gives information on the structure of the solutions. In Figure 8, δ_g is plotted as a function of the LN_2 mole fraction. It can be seen that the Gaussian contribution is negligible for solutions in pure LAr and in pure LN_2. However, in mixed solvents the δ_g value is nonzero, and more so at lower temperatures. It is also seen that at lower temperatures the maximum in the curve shifts to lower concentrations, so that to the left of the maximum the curve has higher absolute slopes than to the right. The asymmetry of the curves can be explained either by preferential solvation with nitrogen, or by the formation of a complex between the solute and N_2. As there appear to be no direct arguments against the preferential solvation hypothesis, we have to conclude that the data in Figure 8 at least do not contradict the formation of a complex.

B. Matrix Isolation Data. Matrix isolation provides a unique means to study very weak associations, because at the very low temperatures used the thermal energy is very low ($k_BT \sim 0.08$ kJ mol^{-1}), and because the solid cages effectively keep the monomers of a trapped complex together.

In Figure 9 we compare the spectral regions of a number of modes of COF_2 of an argon matrix containing only COF_2 (lower traces) with a matrix in which COF_2 and N_2 have been co-condensed (upper traces), both recorded at 10 K. The frequencies observed in the matrices are given in Table 1. The spectra of the matrix containing only COF_2 agrees with previous studies.[25]

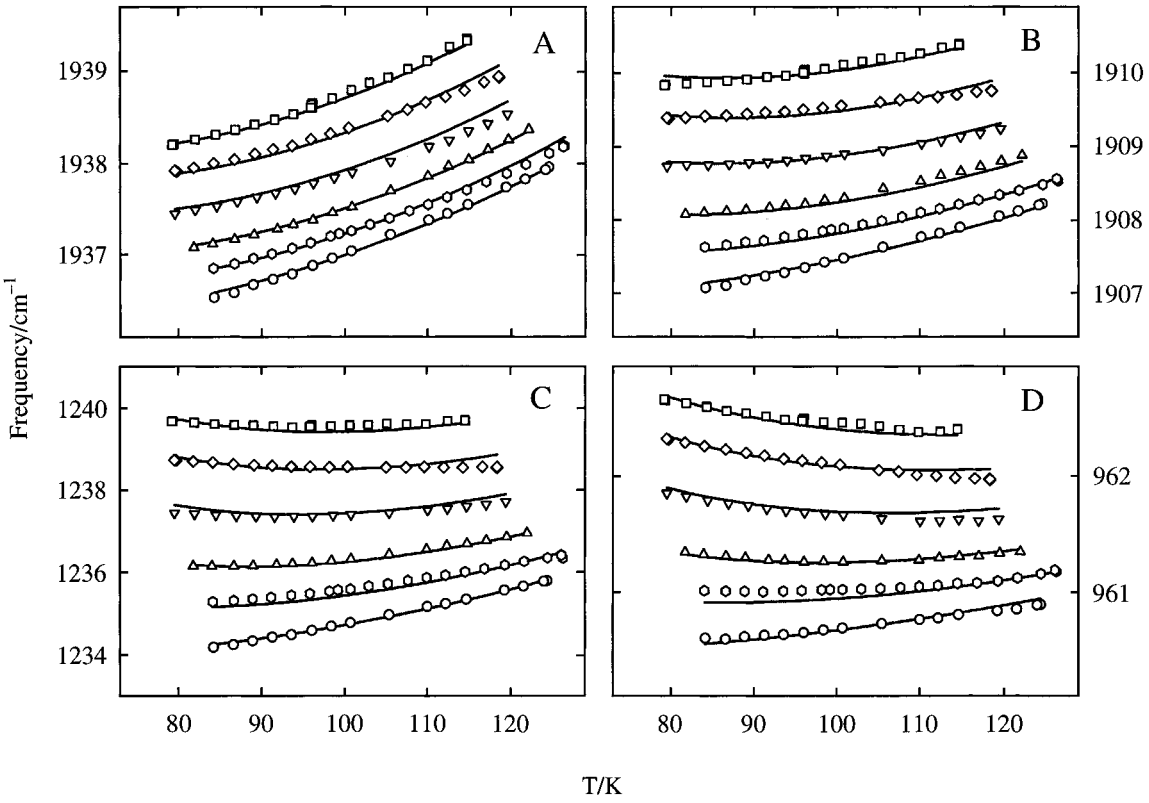

Figure 6. Temperature dependence of the band frequencies of υ_1 (A), $2\upsilon_2$ (B), υ_4 (C) and υ_2 (D) of COF_2 dissolved in LAr/LN_2 mixtures. From bottom to top in each figure, the mole fraction of N_2 equals 0.000, 0.096, 0.222, 0.416, 0.709, and 1.00. The symbols represent the experimental data; the continuous curves were obtained by fitting eq 4 with two adjustable parameters, $\nu_{c,vap}$ and $\alpha_{c,Ar}$.

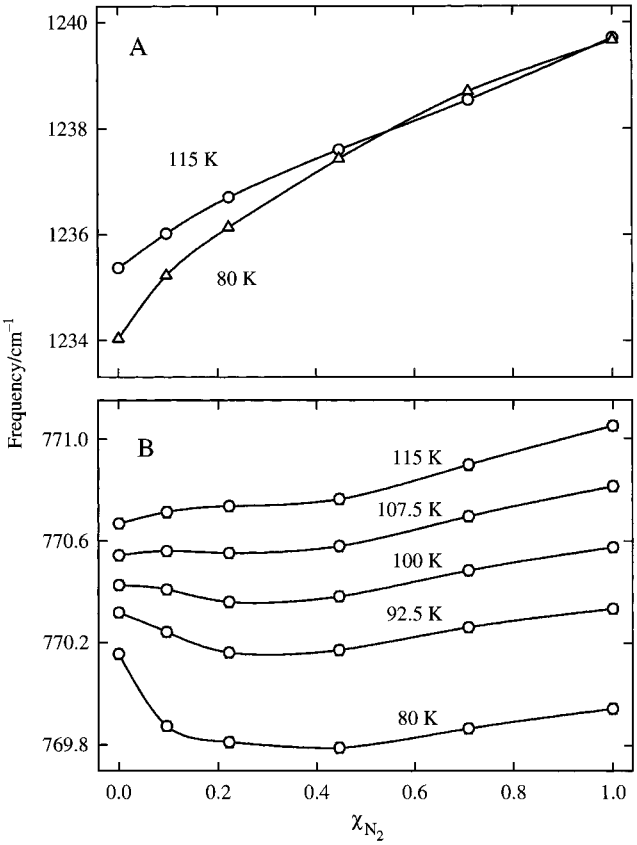

Figure 7. Band frequency of (A) ν_4 and (B) ν_6 of COF_2 as function of the mole fraction of nitrogen in LAr/LN_2 mixtures.

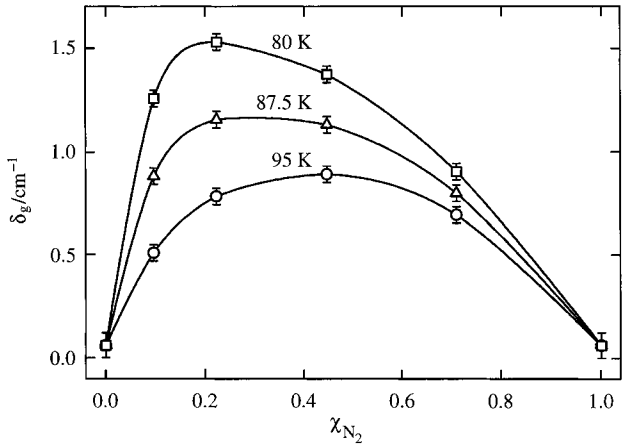

Figure 8. Full width of the Gaussian contribution to the band profile of ν_4 as function of the mole fraction of nitrogen in LAr/LN_2 mixtures, at different temperatures.

It is clear from Figure 9 that in all spectral regions a new band appears in the COF_2/N_2 matrix. Within the uncertainties on the composition of the deposited gas mixtures, the intensities of the new bands increase linearly with the concentration of N_2 in the matrix, and, therefore, the new bands are assigned to a 1:1 complex $COF_2 \cdot N_2$ between the two solutes.

The observed monomer-to-complex shifts are collected in Table 2. The complex bands in Figure 9A−D are blue-shifted from the monomer band. The exception is Figure 9E, which gives the region of ν_6. Here the complex band is red-shifted. This shift and the one in Figure 9C (ν_4) agree with those anticipated above. Hence, the matrix isolation data not only show that a complex can be formed, but also that the complexation shifts agree with what was concluded from the solvent shifts.

C. Ab Initio Calculations. As a consequence of electrostatic and dispersive interactions, the ab initio energy of any pair of neutral molecules, placed at a distance exceeding the sum of

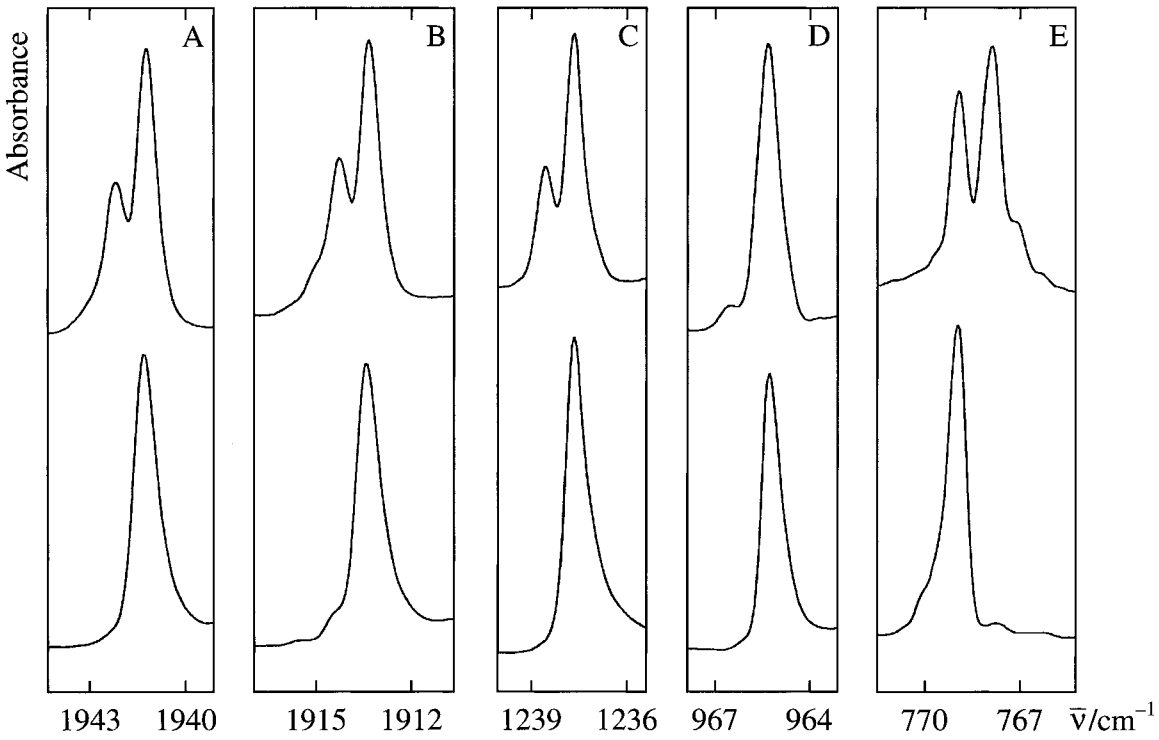

Figure 9. Spectra of COF_2 (lower trace) and of a COF_2/N_2 mixture (upper trace) isolated in an argon matrix at 10 K. For both traces the COF_2:Ar ratio is 1:900. The mole fraction of N_2 in the upper spectrum is 0.003. From (A) to (E) the regions of the ν_1, $2\nu_2$, ν_4, ν_2, and ν_6 modes are given, respectively.

TABLE 2: Calculated and Observed Monomer-to-Complex Frequency Shifts (cm^{-1}) for Some Modes of COF_2

	frequency shift		
mode	ab initio	exp. Ar matrix	exp. cryosolution
ν_1	+1.5	+1.2	+0.7
ν_2	+1.0	+1.5	+3.4
ν_3	+1.4		
ν_4	+2.3	+1.2	+7.7
ν_5	+0.1		
ν_6	−2.3	−1.2	−1.6
$2\nu_2$	(+2.0)[a]	+1.2	+3.7

[a] Estimated at twice the shift of ν_2.

the van der Waals radii, is lower than the sum of the energies of the individual molecules. Hence, such a lowering of the energy does not suffice to prove that the two form an experimentally detectable complex. To do so, the calculations must show that the interaction energy is significantly higher than the thermal energy at which the molecules are investigated experimentally, and must show that, if the experiments are performed in solution, the interaction energy exceeds the solvation energies involved.

The first condition was investigated for a COF_2/Ar and for a COF_2/N_2 pair. Structure optimizations were performed at the MP2/6-311++G(2d,2p) level, starting from different relative positions of the two monomers. For both pairs, the calculations converged into unique structures, in which the Ar or the N_2 is positioned nearly perpendicularly above the carbon atom of COF_2. The ab initio structure of the N_2 complex is shown in Figure 10; the structural parameters of monomers and complex have been collected in Table 3. The latter indicate that the structure of the monomers is hardly changed by the complexation. The small changes that do occur are readily understood from donor−acceptor considerations,[32] and will not be discussed. Figure 10 shows that the nitrogen molecule interacts head-on with the carbon atom of COF_2. This structure is similar

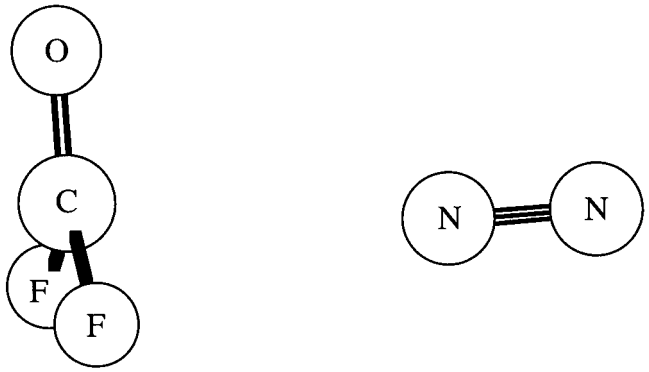

Figure 10. The MP2/6-311++G(2d,2p) ab initio structure of $COF_2 \cdot N_2$.

TABLE 3: MP2/6-311++G(2d,2p) Structural Parameters[a] for COF_2, N_2, $COF_2 \cdot N_2$, and $COF_2 \cdot Ar$

parameter	COF_2	N_2	$COF_2 \cdot N_2$	$COF_2 \cdot Ar$
r(F−C)	1.3194		1.3189	1.3193
r(C=O)	1.1759		1.1760	1.1759
r(C···N)			2.9241	
r(C···Ar)				3.3453
r(N≡N)		1.1128	1.1125	
∠(F−C−O)	126.192		126.177	126.189
∠(F−C−F)	107.618		107.645	107.620
∠(O=C−N)			97.415	
∠(O=C···Ar)				97.538
∠(C···N≡N)			174.057	
τ(N≡N···C=O)			0.0	
τ(F$_1$−C=O,F$_2$)	180.0		179.40	
E/Hartree	−312.596094	−109.363508	−421.963186	−839.640453
μ/Debye	1.14	0.00	1.21	1.14

[a] Bond lengths in Å, bond angles in degrees; the calculated energy for Ar is −527.043067 Hartree.

to that of $BF_3 \cdot N_2$, which has been determined experimentally.[33] This similarity is easily rationalized from the partial charges of the atoms, obtained from a natural bond orbital analysis.[34] For

TABLE 4: Complexation Energies (kJ mol^{-1}) for COF_2·Ar and COF_2·N_2

	COF_2·Ar		COF_2·N_2	
level	ΔE^a	$\Delta E_{corr}{}^a$	ΔE^a	$\Delta E_{corr}{}^a$
MP2	−3.39	−1.21	−9.42	−4.43
MP3	−2.59	−0.35	−7.66	−2.56
MP4(DQ)	−2.46	−0.27	−7.96	−2.99
MP4(SDQ)	−2.68	−0.45	−8.25	−3.23
MP4(SDTQ)	−3.45	−0.97	−9.52	−4.19

[a] ΔE and ΔE_{corr} are the uncorrected and the BSSE-corrected complexation energies, respectively.

BF_3·N_2 the charges are +1.53 e for boron and −0.51 e for the fluorine atoms;[8] for COF_2 the results are +1.16 e for the carbon atom and −0.32 e and −0.52 e for the oxygen and fluorine atoms, respectively. Thus, the electrostatic fields around BF_3 and COF_2 are very similar, which must result in an identical angular geometry of their N_2 complexes.

The influence of higher correlation effects on the energies was investigated by performing single point calculations, for the MP2 geometry, at the MP3 and at several MP4 levels. In addition, in each case the BSSE correction was calculated, using the Boys−Bernardi approach.[26] The same calculations were also performed for the monomers, so that the complexation energy could be obtained by subtracting the monomer energies from those of the complexes. These energies have been collected in Table 4.

With increasing level, the absolute values of the complexation energies can be seen to first decrease, but then increase again. On a relative basis, the uncorrected and BSSE-corrected values, at each level, differ remarkably. For a limited number of van der Waals complexes, experimental complexation energies have been estimated from cryosolution complexation enthalpies.[1−5] The values fell between the uncorrected and corrected ab initio values, from which was concluded that the basis set incompleteness error could not be neglected. In analogy with this, the experimental value for the present complexes also is expected to fall between the uncorrected and corrected ab initio values. In view of the extended basis set used here, it is felt that the experimental energy should be closer to the latter. Therefore, the complexation energy for COF_2·Ar can be estimated to be slightly in excess of 1 kJ mol^{-1}, whereas for COF_2·N_2 the estimate is in excess of 4 kJ mol^{-1}. Experimentally, the compounds are investigated near 100 K, for which k_BT equals 0.83 kJ mol^{-1}. Thus, the complexation energy for COF_2·Ar is of the order of magnitude of k_BT, whereas for COF_2·N_2 it is significantly higher. From this may be concluded that the concentration of COF_2·Ar in LAr will be very small, and the complexes should have negligible influence on the properties of the solution. This is borne out, as was observed above, by the fact that the KBM relation holds for solutions of COF_2 in Ar. On the other hand, the results for the complex with nitrogen support the conclusion that for solutions of COF_2 in LN_2, a reasonable fraction of the COF_2 is complexed into COF_2·N_2.

Some van der Waals complexes exhibit large internal motions, hindered by very low barriers.[35] For such complexes, the ab initio vibrational frequencies, based on the equilibrium structure, will be a poor approximation. Therefore, if ab initio vibrational spectra of COF_2·N_2 are to be of value in the rationalization of our solvent frequency shifts, it must be shown that possible internal motions are hindered by a sufficient barrier. The motion of interest here is the rotation of N_2 around an axis parallel to the COF_2 plane. For this motion, it was assumed that the barrier reaches its maximum when the N_2 molecule is parallel to the COF_2 moiety. Therefore, the structure of a parallel COF_2/N_2 pair was relaxed at the MP2/6-311++G(2d,2p) level. Its energy, uncorrected for BSSE, was found to be 5.99 kJ mol^{-1} above that of the perpendicular pair. This energy difference is the barrier for the internal rotation, and its value amounts to 63% of the total binding energy of the complex. In view of the data in Table 4, this means that the barrier is a multiple of k_BT in our experiments, so that calculating the vibrations at the equilibrium structure should be an acceptable approximation.

The same calculation also serves another purpose. For the complex to be distinguished as a separate species in LN_2, its energy should be substantially lower than the interaction energy between COF_2 and a nonbonded N_2 molecule from the solvation shell. For the latter, the energy of the parallel pair can be taken to be characteristic, so that the above result confirms that also in LN_2 the complex has properties differing from a solvated monomer.

The solution stability of the complex to be expected from the ab initio calculations was obtained by transforming the ab initio estimate of the complexation energy into a solution complexation enthalpy. This was done by adding zero point and thermal contributions, and by correcting for solvent influences. The former were calculated from basic statistical thermodynamics,[36] using the ab initio rotational constants and vibrational frequencies (vide infra) of monomers and complex. Adding these contributions to the lower limit of the expected complexation energy, that is, the BSSE corrected MP4(SDTQ) energy, results in a vapor-phase enthalpy of −2.15 kJ mol^{-1}. From the succes of the KBM relation for LAr solutions, discussed above, it may be expected that a continuum theory of the solvent will result in acceptable solvation energies. Assuming, as before,[1−6] the contribution of electrostatic interactions to be dominant, the solute−solvent interaction free enthalpies for solutions in LAr ($\kappa = 1.46$) were obtained using self consistent isodensity polarized continuum model (SCIPCM) calculations,[37] at the RHF/6-311+G(d,p) level. The free enthalpies were transformed into solute−solvent interaction enthalpies by correcting for entropy contributions.[6,38] The resulting values are 3.16, 0.44, and 2.79 kJ mol^{-1} for COF_2, N_2, and COF_2·N_2, respectively. These values show that, compared with the gas phase, solvation reduces the stability of the complex by 0.81 kJ mol^{-1}. The predicted complexation enthalpy in LAr, therefore, is −1.23 kJ mol^{-1}. This value is very small, and it confirms, in view of what has been said in the *Introduction*, that the vibrational bands of monomers and complex must be expected to coalesce.

The vibrational frequencies of COF_2 and COF_2·N_2 calculated at the MP2/6-311++G(2d,2p) level, are included in Table 1. Table 2 compares the ab initio complexation shifts with the matrix isolation data. The ab initio calculations can be seen to reproduce the directions of the complexation shifts observed in the matrix, including those anticipated above for ν_4 and ν_6. Some quantitative discrepancy between the ab initio and the matrix isolation values is not surprising, taking into account the possible perturbations by the argon matrix.

D. Calculation of the Solvent Frequency Shifts. The equilibrium constant K_{eq} of a 1:1 complex is defined by the following equations:

$$K_{eq} = \frac{x_c}{x_m \times x_{N_2}} \tag{2a}$$

$$K_{eq} = \exp\left(\frac{-\Delta H^o}{RT} + \frac{\Delta S^o}{R}\right) \tag{2b}$$

in which x_c, x_m, and x_{N_2} are the mole fractions of COF_2·N_2, of monomer COF_2, and of N_2, respectively, and ΔH^o and ΔS^o are the complexation enthalpy and entropy, repectively.

Essential to our model is that, similar to what is done in studies on preferential solvation,[39−44] we postulate that the observed position of a band, ν, is the weighted average of the frequencies of monomer, ν_m, and complex, ν_c:

$$\nu = (\nu_m x_m + \nu_c x_c)/(x_m + x_c) \quad (3)$$

Combining eqs 2a and 3 leads to:

$$\nu = (\nu_m + \nu_c K_{eq} x_{N_2})/(1 + K_{eq} x_{N_2}) \quad (4)$$

Because in our experiments x_{N_2} is much larger than x_m, x_{N_2} in eqs 2 and 4 can be considered to be the analytical mole fraction of N_2 in the system.

The KBM-type relation observed for the bands of COF_2 in LAr can be written as:

$$\nu_m = \nu_{m,vap} + \alpha_{m,Ar} \times \chi \quad (5)$$

where $\nu_{m,vap}$ is the vapor-phase frequency of the monomer, $\alpha_{m,Ar}$ is a constant, and χ is the Kirkwood function of the solvent. It appears reasonable to assume that for the frequency of the monomer, and of the complex, in liquid nitrogen similar relations hold:

$$\nu_m = \nu_{m,vap} + \alpha_{m,N_2} \times \chi \quad (6a)$$

$$\nu_c = \nu_{c,vap} + \alpha_{c,N_2} \times \chi \quad (6b)$$

Whereas the parameter $\alpha_{m,Ar}$ can be obtained from KBM plots as those shown in Figures 4 and 5, the constants $\nu_{c,vap}$, α_{m,N_2} and α_{c,N_2} have to be treated as unknowns.

Next, we want to describe the behavior of the vibrational frequencies for mixed solutions. It was remarked above that for the present solvents the solute/solvent interactions are dominated by the pairwise interactions. Within the pairwise approximation, and neglecting effects of preferential solvation, elementary considerations show that for mixed solvents the frequencies must obey the relations:

$$\nu_m = \nu_{m,vap} - [\alpha_{m,Ar}(1 - x_{N_2}) + \alpha_{m,N_2} x_{N_2}] \times \chi \quad (7)$$

$$\nu_c = \nu_{c,vap} - [\alpha_{c,Ar}(1 - x_{N_2}) + \alpha_{c,N_2} x_{N_2}] \times \chi$$

At this stage it must be remarked that the relative permittivities κ, and, therefore, the Kirkwood function χ, have not been determined experimentally for mixtures of LAr and LN_2. They have been calculated as:

$$\chi = \kappa_{LN_2}\, \kappa_{LAr}/[\kappa_{LN_2}(1 - x_{N_2}) + \kappa_{LAr}\, x_{N_2}] \quad (8)$$

The eqs 2b and 7 can be substituted in eq 4, which leads to a relation between the observed frequency ν and a set of six unknown constants: $\nu_{c,vap}$, α_{m,N_2}, $\alpha_{c,Ar}$, α_{c,N_2}, $\Delta H°$ and $\Delta S°$. For each vibrational band studied, the total number of data points, obtained at various temperatures and compositions of the solvent, is 114, which should be ample to reliably fit the unknowns to the experimental data. Such a fitting, using a minimization algorithm based on the approach of ref 45, was performed for ν_1, ν_2, ν_4, ν_6, and $2\nu_2$. For ν_6, the maximum distance between the frequencies in LAr and LN_2 does not exceed 0.4 cm^{-1} (Figure 1). This shows that the frequency of ν_6 in LN_2 is hardly affected by the complexation. Therefore, the parameters obtained from fitting of ν_6 are unreliable. For instance, the value of $\Delta H°$ obtained from ν_6 exceeds the average of the values obtained from the other four frequencies by more than a factor of 2 (-3.0 vs -1.4 kJ mol^{-1}). Therefore, the data for ν_6 were not used in the final fittings.

In a first step, all six unknowns were treated as adjustable parameters. With the adjusted parameters, the observed frequencies were calculated using eqs 2b, 7, and 4. Comparison with the experimental values shows that the standard deviations vary from 0.041 cm^{-1} for ν_1 to 0.11 cm^{-1} for ν_4. The values obtained for $\alpha_{m,Ar}$ and α_{m,N_2} were found to be very close, as were those for $\alpha_{c,Ar}$ and α_{c,N_2}. This is not surprising, taking into account the closeness of the KBM lines observed for the different rare gas solvents, Figures 4 and 5. Therefore, in a second series of calculations, it was assumed that $\alpha_{m,Ar} = \alpha_{m,N_2}$, and that $\alpha_{c,Ar} = \alpha_{c,N_2}$. This reduces the number of adjustable parameters to four. With this set, the largest standard deviation obtained was 0.11 cm^{-1} for ν_4, and the smallest was 0.049 cm^{-1} for ν_1. Because these are very similar to the standard deviations for the original set, the reduction in the number of parameters appears to be justified.

The complexation enthalpies $\Delta H°$ obtained from fitting each of the modes were -1.7 (ν_1), -1.7 (ν_2), -1.2 (ν_4), and -1.2 ($2\nu_2$) kJ mol^{-1}. The small scatter in the values evidently supports the model we have used. The average results in a value for $\Delta H°$ equal to $-1.4(3)$ kJ mol^{-1}. This value is in surprisingly good agreement with the above ab initio prediction, -1.23 kJ mol^{-1}.

The average complexation entropy obtained similarly is $-17(4)$ J K^{-1} mol^{-1}. This value is much smaller than the vapor-phase value of -106 J K^{-1} mol^{-1} calculated by statistical thermodynamics[36] from the ab initio frequencies and rotational constants. This shows that for the solutions, fewer solvent molecules are solvated to the complex than to the monomers. The reasons for this are easily understood from geometrical considerations.

For the final calculation, all experimental data were combined in a single set, and the values for $\Delta H°$ and $\Delta S°$ were fixed at the above averages. Thus, in this calculation only the values for $\nu_{c,vap}$ and $\alpha_{c,Ar}$ were adjusted. The standard deviation for this fit ranged from 0.11 cm^{-1} for ν_4 and 0.050 cm^{-1} for ν_1. These values are only marginally higher than those for the original fit, and this is again taken as supporting the model proposed.

The results of the final calculation, that is, the observable frequencies as function of χ, are shown in Figure 6 as continuous curves. It can be seen that the model neatly reproduces the experimental trends. In particular, the model reproduces the minimum in the relation for ν_4, and the negative slope for ν_2 observed in solutions in pure LN_2 (Figure 6C, 6D).

Although in general the agreement with experiment is satisfactory, some discrepancies can be seen, especially near the highest and the lowest temperatures being studied. These must be attributed to the simplifying assumptions made in the model. For instance, the complexation in the system is assumed to be governed by a single equilibrium constant, and this in a very broad concentration range of N_2. Also, the use of the KBM-like eqs 5−7 is an approximation, and, as has been said, the effects of preferential solvation have been neglected.

The complexation shifts, defined as $\nu_{c,vap} - \nu_{m,vap}$, evaluated from the calculation are collected in Table 2. Within the model used, deviations from KBM behavior are attributed to the formation of complexes. It follows that the effect of the latter on an observed frequency in LN_2 must be correlated with the magnitude of the complexation shift. It can be seen in Table 2 that the largest shifts are calculated for ν_4 [+7.7(4) cm^{-1}] and for ν_2 [+3.4(2) cm^{-1}]. In agreement with this, the LN_2 plots

for these modes in Figures 4 and 5 show the strongest non-KBM behavior.

A qualitative agreement of these data with the results of the matrix isolation spectra and the MP2 calculations, also included in Table 2, can be seen: a negative shift is observed for the ν_6 mode only. The quantitative agreement is not very good, especially for the ν_4 mode, where the cryosolution value seems to be too high. This discrepancy can be attributed either to approximations of the model, or to the difference between the experimental conditions used in getting the matrix isolation and cryospectroscopic data. The observed complexation shifts apparently follow a systematic trend, as the modes that occur in the plane of the COF_2 monomer shift to higher frequencies upon complexation, while the out-of-plane mode ν_6 shifts to a lower frequency. On a relative basis, however, the shifts are very small, and it appears unjustified to interpret them in terms of simple, qualitative models.

At this point the question of the presence of a 1:2 complex must be raised. It is clear from Figure 10 that a second N_2 can interact via the other side of the carbonyl fluoride moiety. Because of the weakness of the interaction between COF_2 and N_2 in the 1:1 complex, it could be anticipated that the interaction with a second N_2 molecule has a similar strength. If so, the 1:2 complex should also show up in the matrix isolation spectra, where, as can be seen in Figure 9, an important fraction of the COF_2 is deposited as 1:1 complex. However, in these spectra no clear indication for the presence of a 1:2 complex can be found, from which we conclude that its concentration is much lower than expected, maybe as the consequence of an as yet unidentified anticooperative effect. Indirectly, the absence of a significant concentration of 1:2 complexes is supported by the results of the above calculations, in which the larger part of the observed shifts is accounted for by a model in which only a 1:1 complex is considered. Evidently, at the lowest temperatures, the presence of a minor amount of 1:2 complexes may well contribute to the remaining discrepancies referred to above.

The complexation is expected to have a measurable influence on the observed frequencies if a significant fraction of the COF_2 molecules in LN_2 is engaged in complexes. This fraction can be calculated from the equilibrium constant K_{eq}, which was evaluated from the $\Delta H°$ and $\Delta S°$ obtained from the fittings. At 100 K, the value of K_{eq} is 0.7(4). For solutions in pure LN_2, at the concentrations of COF_2 used, x_{N_2} is very nearly equal to 1, so that the value of K_{eq} gives the ratio of the concentrations of complex to monomer: it is clear that, indeed, a significant fraction of the COF_2 molecules is complexed.

The observed complexation shifts apparently follow a systematic trend, as the modes that occur in the plane of the COF_2 monomer shift to higher frequencies upon complexation, while the out-of-plane mode ν_6 shifts to a lower frequency. On a relative basis, however, the shifts are very small, and it appears unjustified to interpret them in terms of simple, qualitative models.

Conclusions

Analysis of the infrared spectra shows that the frequencies of COF_2 dissolved in LAr follow predictions from continuum solvent theories, whereas deviations are observed for solutions in LN_2. These deviations are attributed to the formation of a complex between COF_2 and N_2, even if no separate bands due to the complex are observed.

A complex between COF_2 and N_2 is observed in a solid argon matrix, and ab initio calculations confirm its possible occurrence in cryosolutions.

A model is proposed in which it is assumed that the observed band frequencies in LN_2 and in mixtures of LAr and LN_2 are a weighted average of the monomer and complex frequencies. The model satisfactorily reproduces the observed temperature and concentration dependence of the spectral bands, and the complexation enthalpy derived from it is $-1.4(3)$ kJ mol^{-1}, in good agreement with extrapolations from the ab initio calculations, and of the right magnitude to give rise to coalescence of complex and monomer bands in the vibrational spectra. The complexation shifts observed in the matrix, and those calculated by ab initio, agree reasonably with those calculated from the model.

The consistency of the obtained data supports the validity of our phenomenological model, and shows that even when separate bands due to the complex are not observed, important information on the complex can be abstracted from the spectra.

Acknowledgment. W.A.H. thanks the Fund for Scientific Research (FWO, Belgium) for an appointment as Postdoctoral Fellow. The FWO is also thanked for financial help toward the spectroscopic equipment used in this study. Support by the Flemish Community, through the Special Research Fund (BOF) is gratefully acknowledged. The authors are grateful to Dr. V. V. Gorbatchuk and Prof. B. N. Solomonov for fruitful discussions.

References and Notes

(1) Sluyts, E. J.; Van der Veken, B. J. *J. Am. Chem. Soc*. **1996**, *118*, 440.

(2) Herrebout, W. A.; Van der Veken, B. J. *J. Am. Chem. Soc*. **1997**, *119*, 10446.

(3) Van der Veken, B. J.; Sluyts, E. J. *J. Am. Chem. Soc*. **1997**, *119*, 11516.

(4) Herrebout, W. A.; Everaert, G. P.; Van der Veken, B. J.; Bulanin, M. O. *J. Chem. Phys*. **1997**, *107*, 8886.

(5) Everaert, G. P.; Herrebout, W. A.; Van der Veken, B. J.; Lundell, J.; Räsänen, M. *Chem. Eur. J*. **1998**, *4*, 321.

(6) Stolov, A. A.; Herrebout, W. A.; Van der Veken, B. J. *J. Am. Chem. Soc*. **1998**, *120*, 7310.

(7) Tokhadze, K. G. In *Molecular Cryospectroscopy*; Clark, R. J. H.; Hester, R. E., Eds.; Wiley: Chichester, 1995; p 151.

(8) Herrebout, W. A.; Van der Veken, B. J. *J. Am. Chem. Soc*. **1998**, *120*, 9921.

(9) Buckingham, A. D. *Proc. R. Soc. London Ser A* **1958**, *248*, 169; *ibid. Ser A* **1960**, *255*, 32; *Trans. Faraday Soc.* **1960**, *56*, 753.

(10) Schweizer, K. S.; Chandler, D. *J. Chem. Phys.* **1982**, *76*, 2296.

(11) Zakin, M. R.; Herschbach, D. R. *J. Chem. Phys.* **1988**, *89*, 2380.

(12) Lee, Y. T.; Wallen, S. L.; Jonas, J. *J. Phys. Chem*. **1992**, *96*, 4282.

(13) Devendorf, G. S.; Ben-Amotz, D. *J. Chem. Phys*. **1996**, *104*, 3479.

(14) Ben-Amotz, D., Herschbach, D. R. *J. Phys. Chem*. **1993**, *97*, 2295.

(15) Tomasi, J.; Perisco, M. *Chem. Rev*. **1994**, *94*, 2027.

(16) Wong, M. W.; Wiberg, K. B.; Frisch, M. J. *J. Chem. Phys*. **1991**, *95*, 8991.

(17) Rivail, J.-L.; Rinaldi, D.; Dillet, V. *Mol. Phys*. **1996**, *89*, 1521−1529.

(18) Luck, W. A. P.; Klein, D. *J. Mol. Struct.* **1996**, *381*, 83.

(19) Kolling, O. W. *J. Phys. Chem*. **1996**, *100*, 16087.

(20) Bulanin, M. O.; Orlova, N. D.; Zelikina, G. Ya. In *Molecular Cryospectroscopy*; Clark, R. J. H.; Hester, R. E., Eds.; Wiley: Chichester, 1995; p 47.

(21) Reichardt, C. *Solvents and Solvent Effects in Organic Chemistry*, 2nd ed.; VCH Publishers: Weinheim, 1988.

(22) Josien, M.-L.; Fuson, N. *J. Chem. Phys*. **1954**, *22*, 1169.

(23) Van der Veken, B. J.; De Munck, F. *J. Chem. Phys*. **1992**, *97*, 3060.

(24) Frisch, M. J.; Trucks, G. W.; Schlegel, H. B.; Gill, P. M. W.; Johnson, B. G.; Robb, M. A.; Cheeseman, J. R.; Keith, T.; Petersson, G. A.; Montgomery, J. A.; Raghavachari, K.; Al-Laham, M. A.; Zakrzewski, V. G.; Ortiz, J. V.; Foresman, J. B.; Cioslowski, J.; Stefanov, B. B.; Nanayakkara, A.; Challacombe, M.; Peng. C. Y.; Ayala, Y.; Chen, W.; Wong, M. W.; Andres, J. L.; Replogle, E. S.; Gomperts, R.; Martin, R. L.; Fox, D. J.; Binkley, J. S.; Defrees, D. J., Baker, J.; Stewart, J. P.; Head-

Gordon, M.; Gonzalez, C.; Pople, J. A. *Gaussian94, Revision B.2*; Gaussian, Inc.; Pittsburgh, PA, 1995.

(25) Peng, C.; Ayala, P. Y., Schlegel, H. B.; Frisch, M. J. *J. Comput. Chem*. **1996**, *17*, 49.

(26) Boys, S. B.; Bernardi, F. *Mol. Phys*. **1970**, *19*, 553.

(27) Mallinson, P. D.; McKean, D. C.; Holloway, J. H.; Oxton, I. A. *Spectrochim. Acta* **1975**, *31A*, 143.

(28) Belozerskaya, L. P.; Zhigula, L. A.; Shchepkin, D. N. *Opt. Spectrosc*. (USSR), **1979**, *47*, 267.

(29) Van der Veken, B. J. *J. Phys. Chem*. **1996**, *100*, 17436.

(30) Stone, A. J. *The Theory of Intermolecular Forces*; Clarendon Press: Oxford, 1996; p 141.

(31) Rothschild, W. G. *J. Chem. Phys*. **1976**, *65*, 455.

(32) Gutman, V. *The Donor Acceptor Approach to Molecular Interactions*; Plenum Press: New York, 1988.

(33) Janda, K. C.; Bernstein, L. S.; Steed, J. M.; Novick, S. E.; Klemperer, W. *J. Am. Chem. Soc*. **1978**, *100*, 8074.

(34) Reed, A. E.; Curtiss, L. A.; Weinhold, F. *Chem. Rev*. **1988**, *88*, 899.

(35) Bauder, A. In *Structures and Conformations of Non Rigid Molecules*; Laane, J.; Dakkouri, M.; Van der Veken, B.; Oberhammer, H., Eds.; Kluwer Academic Publishers: Dordrecht, 1993.

(36) Knox, J. H. *Molecular Thermodynamics. An Introduction to Statistical Thermodynamics for Chemists*; Wiley-Interscience: London, 1971.

(37) Foresman, J. B.; Keith, T. A.; Wiberg, K. B.; Snoonian, J.; Frisch, M. J. *J Phys. Chem.* **1996** *100*, 16098.

(38) The value quoted in ref 6 for the correction factor to be applied to the free enthalpy for solutions in LAr, 1.51, is incorrect, the true value being 1.61.

(39) Acree, W. E.; Powell, J. R. *Phys. Chem. Liq*. **1995**, *30*, 63.

(40) Acree, W. E.; Tucker, S. A.; Wilkins, D. C. *J. Phys. Chem*. **1993**, *97*, 11199.

(41) Roses, M.; Rafols, C.; Ortega, J.; Bosch, E. *J. Chem. Soc., Perkin Trans*., **1995**, *1607*.

(42) Szpakowska, M.; Nagy, O. B. *J. Phys. Chem*. **1989**, *93*, 3851.

(43) Jamroz, D.; Stangret, J.; Lindgren, J. *J. Am. Chem. Soc*. **1993**, *115*, 6165.

(44) Novikov, V. B.; Stolov, A. A.; Gorbatchuk, V. V.; Solomonov, B. N. *J. Phys. Org. Chem*. **1998**, *11*, 283.

(45) Press: W. H., Teukolsky, S. A.; Vetterling, W. T., Flannery, B. P. *Numerical Recipes in FORTRAN*, 2nd Ed.; Cambridge University Press: Cambridge, 1992; p 665.